DISTRIBUTED STRAIN SENSING FOR COMPOSITES BY EMBEDDED FBG SENSORS

Hideaki Murayama*, Kazuro Kageyama*, Shunichi Kobayashi*, Isamu Ohsawa*, Kiyoshi Uzawa*, Makoto Kanai*, Soohyun Eum*, Gakuro Akiyama*, Kohei Ohara*, Hirotaka Igawa, Tokio Kasai**, Isao Yamaguchi**, and Takehiro Shirai *****

***The University of Tokyo, 7-3-1, Hongo, Bunkyo-ku, Tokyo, Japan**

****Japan Aerospace Exploration Agency, 6-13-1 Osawa, Mitaka-shi, Tokyo, Japan**

*****Lazoc Inc. , 3-40-9, Hongo, Bunkyo-ku, Tokyo, Japan**

Keywords: *Distributed measurement, Fiber Bragg grating, OFDR, Structural health monitoring, Smart Structure*

Abstract

We have developed a new distributed strain measurement system with a long gauge FBG sensor based on Optical Frequency Domain Reflectometry (OFDR), which enables us to measure strain at an arbitrary position along the FBG sensor with the high spatial resolution of sub-millimeter order. Such performance of high resolution sensing can be applied to health monitoring of a structure which may have stress concentration. In this study, we implemented experiments to measure the strain distributions by embedded FBG sensors on the FRP specimen which was subjected to tensile loads. Then, we could successfully measure the strain distribution and monitor stress concentration.

1 Introduction

Fiber reinforced plastics (FRP) has been widely used in a variety of applications in sectors such as the aerospace, automobile and marine industries because of the high specific strength and stiffness. However, as they are often employed in severe operating environments, it is necessary to monitor structural conditions to secure the integrity of the FRP structures.

Optical fiber sensors are broadly accepted as a promised candidate of sensor components in structural health monitoring (SHM) systems for a structure made of FRP [1], because they can be alternatively installed into the structure by embedding [2] or bonding [3] without degradation of the structural performance or integrity.

Among them, Fiber Bragg Grating (FBG) sensors with an interrogating system, such as wavelength division multiplexing (WDM), have been employed to apply quasi-distributed measurement systems to SHM. FBG sensors can measure strain precisely by WDM if the strain isn't varying within the gauge length of FBG. However, if the strain isn't uniform within the gauge length, we cannot obtain precise strain from the measurement system based on WDM because of shape distortion of the reflection spectrum, and we cannot also measure strain distribution along the FBG sensor by such conventional interrogating methods.

On the other hand, various techniques for fully-distributed sensing have been proposed in recent years. By using Brillouin Optical Time Domain Reflectometry (BOTDR), we can measure strain at an arbitrary position along an optical fiber [4]. So, strain distribution of a structure can be effectively monitored by it. It, however, is difficult to detect the initial damage which may lead to stress concentration and then critical failure, because the spatial resolution of the distributed sensing system with OTDR, which is ordinarily 1m, is inadequate to monitor strain changing in a local area [5]. Therefore, in order to monitor strain distribution of a structure effectively and detect damage or degradation accurately, it is expected to apply a distributed strain sensor with the higher spatial resolution to SHM.

Recently, we have developed a new distributed strain measurement system with a long gauge FBG sensor based on Optical Frequency Domain Reflectometry (OFDR), which enables us to measure strain at an arbitrary position along the FBG sensor

with the high spatial resolution of sub-millimeter order [6]. In this study, we implemented experiments to measure the strain distributions by embedded FBG sensors on the FRP specimen which was made by vacuum assisted resin transfer molding (VaRTM) and then subjected to tensile loads.

2 Distributed Sensing Using OFDR

2.1 Fiber Bragg Grating Sensor

The basic principle of measurement used FBG sensor is to monitor the shift in wavelength of Bragg signal with the change in the measurand. The Bragg wavelength is given by

$$\lambda_B = 2n_{eff}\Lambda \qquad (1)$$

where Λ is the grating pitch and n_{eff} is the effective index of the core. As the measurand, such as strain or temperature, changes Λ or n_{eff}, the Bragg wavelength, λ_B, also changes. Fig. 1 shows the shift of Bragg wavelength with strain or temperature.

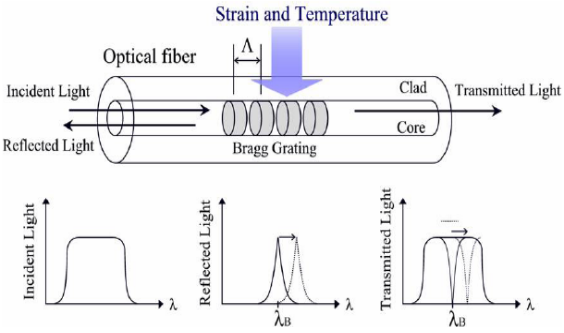

Fig. 1. Shift of the Bragg wavelength with strain or temperature

The measured strain response at constant temperature is found to be [7]

$$\frac{1}{\lambda_B}\frac{\partial \lambda_B}{\partial \varepsilon} = 0.78\times 10^{-6} \quad \mu\varepsilon^{-1} \qquad (2)$$

2.2 Measurement System with OFDR

The sensing system in this study consists of a wavelength tunable laser, two photodiode detectors (D1, D2), three broadband reflector (R1, R2, R3), three 3dB couplers (C1, C2, C3), a long gauge FBG and desktop computer with A/D converter. The layout of the sensing system is shown in Fig. 2.This is similar to that of Ref.[8] expect for the long gauge FBG.

The signal at D1 is given by the following equation.

$$D_1 = 2\{1+\cos(2n_{eff}L_R k)\} \qquad (3)$$

where n_{eff} is the effective index, L_R is the path difference of the two paths through the interferometer, and k is the wavenumber of the light and is related to the wavelength λ and given by the following equation.

$$k = \frac{2\pi}{\lambda} \qquad (4)$$

As the laser tuned, the light intensity observed by D1 varies in a cycle depending on a wavenumber change, Δk, of the following equation [8].

$$\Delta k = \frac{\pi}{n_{eff}L_R} \qquad (5)$$

This signal acts as trigger for data acquisition at D2. Therefore, by using the signal of D1 as trigger, we can sample the signal of D2 with the constant wave number interval and the signal is given by

$$D_2 = R_i(k)\cos(2n_{eff}L_i k) \qquad (6)$$

where R_i is the spectrum of the i'th grating and L_i is the path difference of the corresponding i'th interferometer. The waveform of signal D2 which is obtained from a 100 *mm* gauge FBGT with uniform strain is shown in Fig. 3.

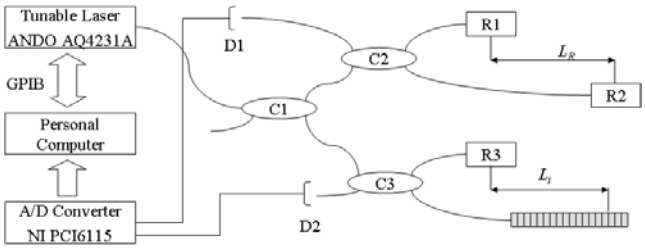

Fig. 2. Measurement system with OFDR

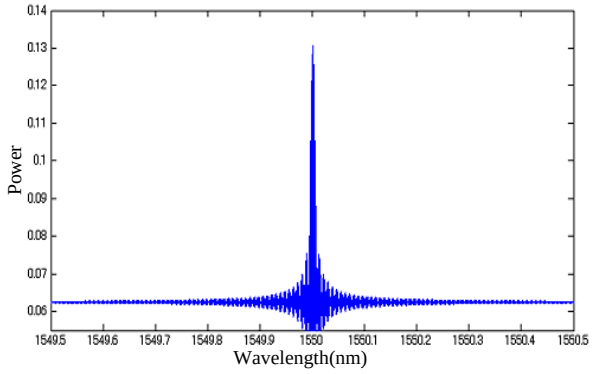

Fig. 3. Waveform of Signal D2

D2 acquires the signal depending on the intensity of the reflected light that includes oscillation with some frequencies corresponding on L_i. Then, by applying Fourier transform analysis with a sliding window to the signal we could map the strain profile along the long gauge FBG from a spectrogram as shown in Fig. 4. The axis of abscissas represents wavelength and the axis of ordinates represents position. In this spectrogram, we can see uniform reflection spectra along the FBG (1.00 *m* to 1.10 *m*).

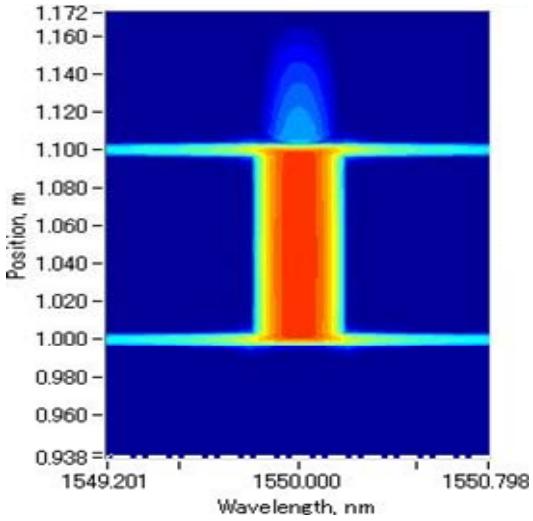

Fig. 4. Spectrogram

In this study, we determined the center of wavelength by calculating the center of the full width at half maximum (FWHM) of a reflection spectrum at each position in the spectrogram as shown in Fig. 5.

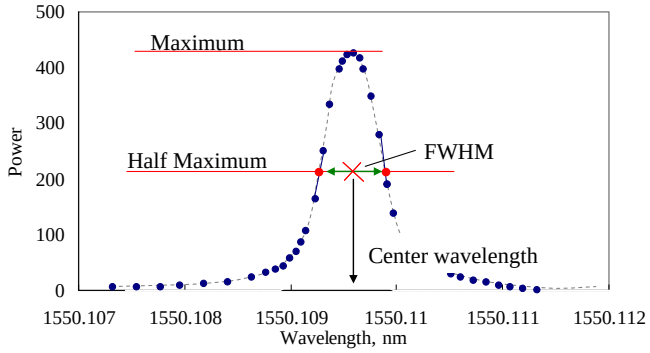

Fig. 5. Spectrum of a position and how to calculate the center wavelength

3 Experimental Details

3.1 Test Specimen

The test specimen was made by VaRTM. A typical VaRTM setup is shown in Fig. 6. Vacuum acts as driving forces to draw resin into the preform, compact the preform and remove air from resin and mold cavity. A mold is sealed by a vacuum bag film and tacky sealant tapes. Resin is infused to the preform through a spiral tube from the inlet port by vacuum pressure and distributed into the whole preform smoothly by a porous resin flow distribution media. An extracted resin is flowed out to vacuum port through another spiral tube. A peel ply is inserted on the preform in order to peel off a porous resin flow distribution media and the vacuum film after curing.

Fig. 7 (a) shows the test specimen made by VaRTM. Three FBGs were embedded in the GFRP laminate and another one was located out of the laminate as a reference sensor. The stacking sequence of the fabrics and the long gauge FBGs was chosen as [fabric4/ {0}FBG 1/fabric6/ {0}FBG 3/fabric6/{0}FBG 2/fabric4]. Each FBG was embedded with 10 *mm* interval at the center of specimen on its length direction. The gauge length of embedded FBGs was 100 *mm* and the one of the reference FBG was 50 *mm*. FBG 1 and 2 were embedded on the 4th and the 16th plies respectively and were exposed to preform and resin directly. On the other hand, FBG 3 was inserted in the tube so that FBG 3 was a strain free condition to compensate temperature for the data which obtained from FBG 1 and 2. FBG 4 also installed to use as a reference. Two strain gauges were also bonded on the both side above FBG at 40 *mm* interval. It was subjected to tensile loads by a tensile testing machine shown in Fig. 8.

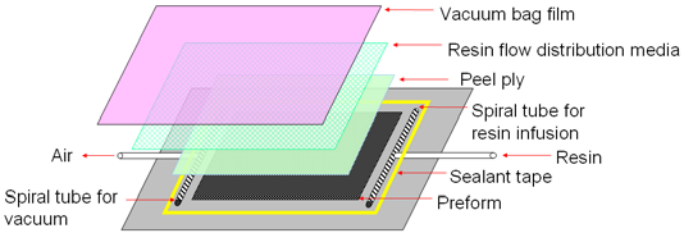

Fig. 6. VaRTM set-up

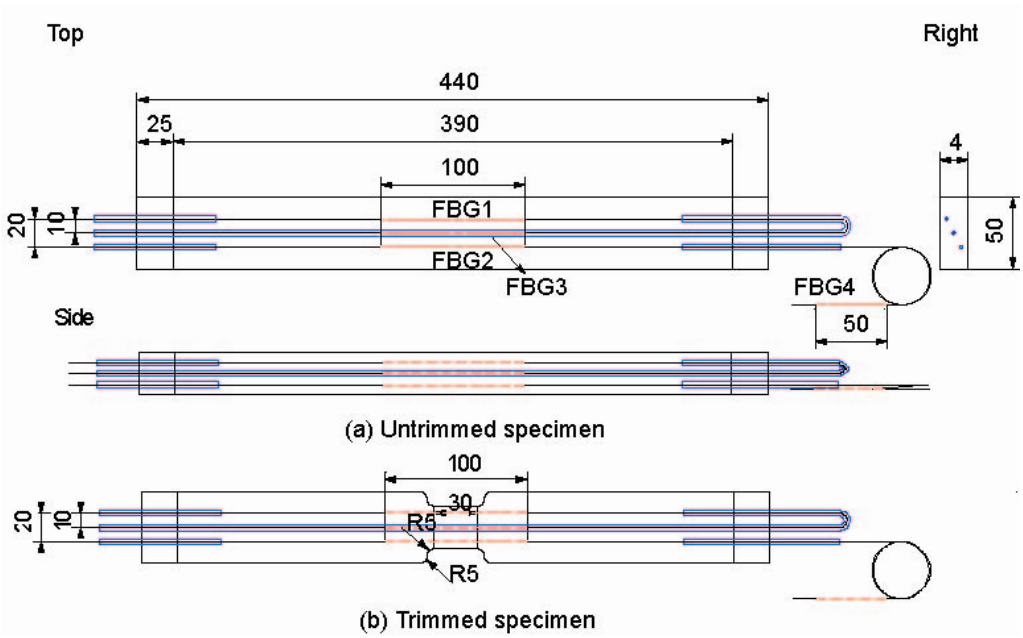

Fig. 7. Specimen configuration

(a) Tensile Testing Machine (b) Test Specimen

Fig. 8. Experimental set-up

3.2 Tensile Test

We measured the strain by two FBG at each increment of about 100 $\mu\varepsilon$ under static load. Signals at D2 were acquired by the A/D converter and stored in the desk top computer. The spectrograms calculated by applying time-frequency analysis to the signal of D2 at FBG 1 are shown in Fig. 9. The left one represents the distribution of the wavelength spectra under no load, and the right one represents the distribution of the wavelength spectra under the tensile load, respectively. In these spectrograms, we can see reflection spectra along the FBG 1 (3.28 *m* to 3.38 *m*) and the center wavelengths are positively shifted due to the tensile load.

Strain distributions calculated by Eq. (2) are shown in Fig. 10. We used the center wavelength under no load (0 *kN*) as reference to determine the shift of that. The graph legends are the strain value measured by the strain gauge. We can see that the agreement between strains measured by the long gauge FBG and the strain gauge is excellent and the FBG sensor is able to monitor the distribution along the sensor. It can be seen that the strain distribution of FBG 1 is slightly convex upward and that of FBG 2 is convex downward in contrast. It could have been caused by the initial condition that the specimen was slightly bended.

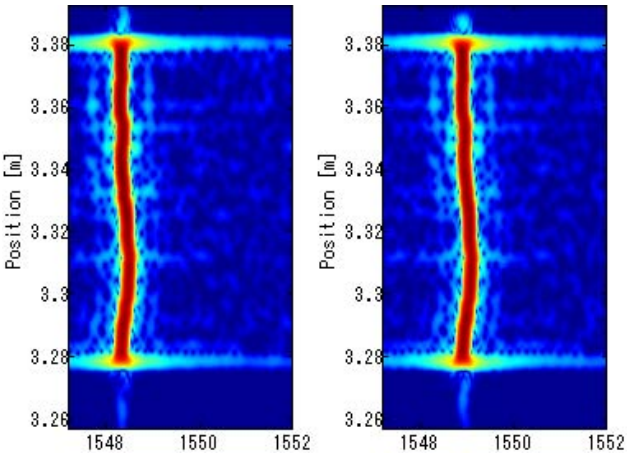

(a) under no load (b) under a tensile load

Fig. 9. Spectrograms of FBG 1 embedded in the untrimmed specimen

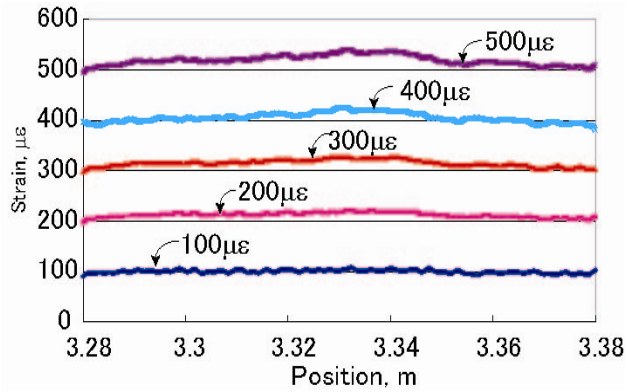

(a) FBG1

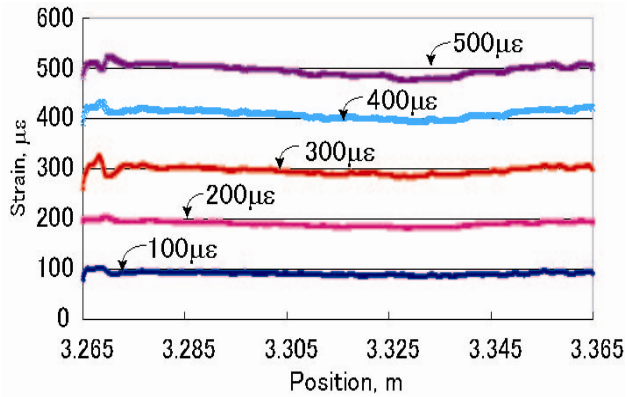

(b) FBG2

Fig. 10. Strain distributions of FBGs embedded in the untrimmed specimen

3.3 Stress Concentration

After a load series test, the specimen was trimmed to deteriorate the stiffness as shown in Fig. 7 (b). The specimen was subjected to the tensile load from 0 *kN* to 1.20 *kN*.

We measured the strain by two FBG sensors under static load (0, 0.24, 0.48, 0.72, 0.96, 1.20 *kN*). The spectrograms calculated by applying time-frequency analysis to the signal of D2 at FBG 1 are shown in Fig. 11. In these spectrograms, we can see the center wavelengths are positively shifted in the sensing region (5.45 *m* to 5.55 *m*) overall. In addition, we can see the center wavelengths around the center of sensing region are strongly shifted because of stiffness degradation.

Strain distributions calculated by Eq. (2) are shown in Fig. 12. The solid lines represent the strain distributions calculated by finite element method (FEM). We can see the good agreement between strain distributions measured by the long gauge FBG and strain distributions calculated by FEM.

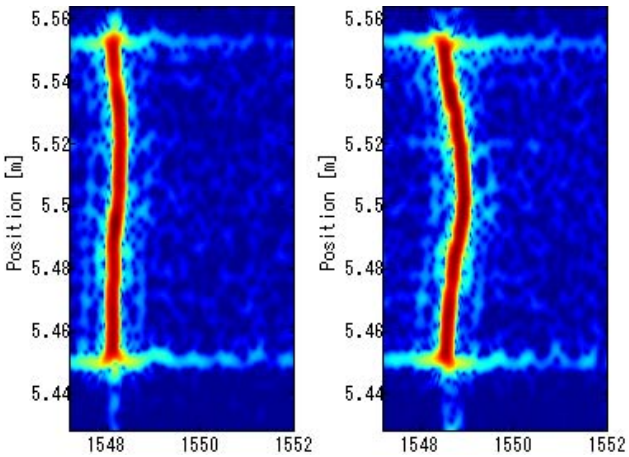

(a) under no load (b) under a tensile load

Fig. 11. Spectrograms of FBG 1 embedded in the trimmed specimen

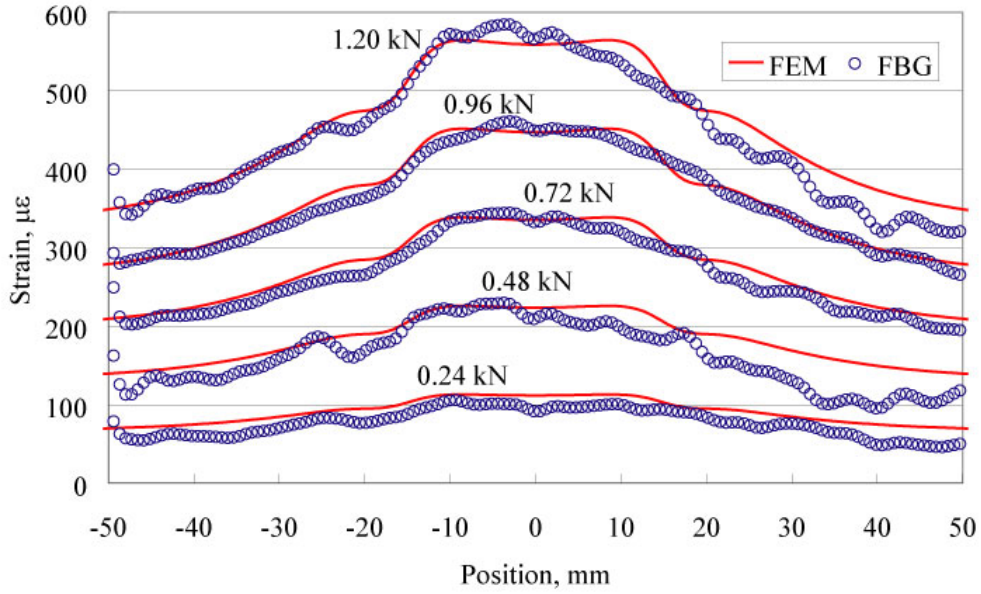

Fig. 12. Strain distributions of FBG 1 embedded in the trimmed specimen

4 Conclusion

We applied the strain measurement system based on OFDR to measuring strain distribution on the FRP specimen by the embedded FBG sensors and we could successfully measure the uniform strain. Also, we could monitor stress concentration on the trimmed specimen. Furthermore, we can use this embedded sensor to monitor the flow or the cure of the resin in manufacturing FRP. In conclusion, it is suggested that this sensing technique can apply to SHM of composite structures made by VaRTM.

References

[1] Eric Udd 1995. “Fiber Optic Smart Structures”, Wiley-Interscience,

[2] G Zhou1, L M Sim, Damage detection and assessment infibre-reinforced composite structures with embedded fibre optic sensors, Smart Materials and Structures, Volume 11, pp. 925-939, Number 2002

[3] Hideaki Murayama, Kazuro Kageyama, Isao Kimpara, Akiyoshi Shimada, Hiroshi Naruse, Health monitoring of large composite structures by using fiber optic distributed strain sensors - Experiences at America`s Cup 2000 -, Journal of Advanced Science, vol.12, no.3, pp.298-302, 2000

[4] T. Kurashima, T. Horiguchi, H. Izumita, S. Furukawa, and Y.Koyamada, Brillouin optical-fiber time domain reflectometry, IEICE Trans. Commun. E76-B, 382–390 ,1993

[5] Hideaki Murayama, Kazuro Kageyama, Hiroshi Naruse, Akiyoshi Shimada, Distributed Strain Sensing from Damaged Composite Materials Based on Shape Variation of the Brillouin Spectrum, Journal of Intelligent Material Systems and Structures, vol.15, pp.17-25, Jan.2004

[6] Hirotaka Igawa, Hideaki Murayama, Tokio Kasai, Isao Yamaguchi , Kazuro Kageyama, Keiichi Ohta, Measurements of strain distributions with a long gauge FBG sensor using optical friquency domain reflectometry, Proc. of SPIE, Vol. 5855, pp.547-550, May 2005, Belgium

[7] Alan D.Kersey et al: Fiber Grating Sensors, Journal of Lightwave Technolog, Vol.15, No.8, 1997

[8] B. Childers, M. E. Froggatt, S. G. Allison, T. C. Moore, D. A. Hare, C. F. Batten and D. C. Jegley 2001. “Use of 3000 Bragg grating strain sensors distributed on four eight-meter optical fibers during static load tests of a composite structure”, Proc. of SPIE, vol. 4332, pp. 133-142.